ELSEVIER

Journal of Hazardous Materials B103 (2003) 107–123

Journal of Hazardous Materials

www.elsevier.com/locate/jhazmat

Pyrolysis kinetics of electronic packaging material in a nitrogen atmosphere

Tzong-Horng Liou*

Department of Chemical Engineering, Hsiuping Institute of Technology, Taichung 412, Taiwan, ROC

Received 14 April 2003; received in revised form 9 July 2003; accepted 10 July 2003

Abstract

The kinetics of pyrolysis of electronic packaging material are investigated under various heating rates (5, 10, 15, 20 K/min) in an inert atmosphere using a thermogravimetric analysis (TGA) technique. The pyrolysis characteristics of samples are examined by SEM, XRD, FTIR, ICP-MS and EA. The effect of heating condition on the surface area and pore structure of samples is discussed. Two reaction stages are involved for the pyrolysis of electronic packaging material when nitrogen is present in the carrier gas. The corresponding kinetic parameters, including activation energy, pre-exponential factor and reaction order are presented. The apparent activation energies can be divided into three groups. The results will be useful in developing pyrolysis or incineration systems for plastic waste from electronic components.

Keywords: Electronic packaging material; Pyrolysis; Kinetics; Mechanism; Thermogravimetric analysis

1. Introduction

Over the past two decades, the electronic packaging industry has grown very rapidly worldwide. Electronic packaging materials are widely used in the encapsulation of electrical devices such as integrated circuits (IC). Electronic packaging uses resin materials with high silica content (60–80 wt.%), and residual resins generated during the IC packaging process comprise about 30–50 wt.% of the total resin compounds. The waste has been cured with a cross-linking reaction between epoxy resin and hardener in the electronic packaging process. It is hard to melt and decompose, so land-fill is the main method to solve the disposal problem. However, because plastic materials are essentially non-biodegradable, land-fill is currently impracticable. Accordingly, thermal treatment of these materials by

* Tel.: +886-4-24961198; fax: +886-4-24961185.
E-mail address: liouth@mail.hit.edu.tw (T.-H. Liou).

0304-3894/$ – see front matter © 2003 Elsevier B.V. All rights reserved.
doi:10.1016/S0304-3894(03)00244-9

Nomenclature

A	pre-exponential factor (min^{-1})
C	char
E	activation energy (kJ/mol)
f	function of conversion
I, II	intermediates during pyrolysis of resins
k	pyrolysis rate constant (min^{-1})
M	epoxy resin
n	reaction order
P	phenol resin
P/P_0	relative pressure for nitrogen adsorption–desorption
R	gas constant = 8.314 kJ/kmol K
t	pyrolysis time (min)
T	pyrolysis temperature (K)
T_f	final pyrolysis temperature (K)
T_i	initial pyrolysis temperature (K)
T_m	peak temperature (K)
V_1, V_2, V_3, V_4	volatiles
W	weight of sample at time t (mg)
W_0	initial weight of sample (mg)
W_∞	final weight of sample (mg)
X	conversion of electronic packaging material

Greek symbols

β	heating rate (K/min)
Δ	change in property

pyrolysis or incineration is becoming attractive. In recent years, with the rapid growth of IC packaging, pyrolysis-based technology has been considered as a useful approach to solve the growing quantity of waste.

The composition of a typical material used for the IC packaging is epoxy resin, phenol resin, silica and additives. The electronic packaging material is manufactured by premixing these components, then blending, cooling, crushing and tabulating. The tablet is melted by heating to a highly viscous liquid state, and then pressed into a heated mold containing lead-frame strips with their attached ICs. After curing the resin, this mold is cooled to freeze the resin as quickly as possible. The final products are removed from the mold, and the residual resins are recovered after the packaging process [1,2].

Much work has been done on the pyrolysis or burning of thermosetting materials such as epoxy resin [3–6]. However, few studies have been conducted on pyrolysis of resin compounds containing silica, such as electronic packaging material. The kinetics of pyrolysis of electronic packaging materials in inert gas have rarely been investigated. Recently, Liou [7] investigated the thermal decomposition kinetics of electronic packaging material in an

oxidizing atmosphere in which the kinetic parameters and probable reaction mechanism were determined. Iji and Ikuta [8] used the secondary combustion method to recover the combustion exhaust gas, which contains organic bromine compounds, generated in the burning of the electronic packaging material. They also found that the silica recovered from the material can be used as inorganic filler for other electronic components. Budrugeac [9] observed that the major loss of mass during thermal decomposition of glass-reinforced epoxy resin was attributed to formation of volatile products. In addition, the total thermal degradation process is an exothermic reaction.

This research investigates the effect of various heating conditions on the pyrolysis of electronic packaging material. A thermogravimetric analysis (TGA) technique is used to analyze the process of thermal decomposition. The experiments are carried out at various heating rates (5, 10, 15, 20 K/min) with nitrogen as the carrier gas. The kinetic parameters, such as activation energy, pre-exponential factor, and reaction order, as well as the effect of operating variables on the properties of the product are extensively investigated. A mechanism is also developed to account for the experimental results.

These results should be useful for the rational design or operation of pyrolysis or incineration systems in which plastic waste from electronic components are involved. In addition, the silica recovered from the electronic packaging material is also a source of silicon for manufacture of other ceramic materials, such as silicon nitride powder [10,11].

2. Experimental

2.1. Material used and sample preparation

The samples of electronic packaging material used in the study were supplied by an electronic packaging mill (Siliconware Precision Co., Taiwan), and their basic constituents and properties are listed in Table 1. The samples were washed well with distilled water to remove dust and dried in an air oven. High-purity (99.99%) nitrogen gas (San-Fu Chem. Co.) was used as the purge gas for all pyrolysis experiments.

The water-rinsed samples were pulverized, and then were ground and screened through an ASTM standard sieve to obtain the desired grain sizes (325 mesh size).

Table 1
Basic constituents and properties of electronic packaging material

Material family	Composition	Function	Weight (%)
Sealant	Epoxy resin	Curing, adhesive, waterproof, insulate	10–15
Hardener	Phenol resin	To cure by cross-linking	10–15
Filler	Silica powder	Minimize the shrinkage of resin, improve mechanical properties	60–80
Flame retardant	Antimony trioxide	Inorganic fire-resistant	1–5
Flexibility additive	Silicone elastomer	Prevent cracking	2–4
Releasing agent	Carnauba wax	Release from mold	0.2–0.3
Coloring agent	Carbon black	Coloring	0–0.5
Accelerator	Tertiary amine	Promote the hardening rate	0.2–0.3

2.2. Apparatus and procedures of pyrolysis

The experiments on the kinetics of the pyrolysis reaction were carried out using a thermogravimetric analysis technique, and the basic scheme of the experimental setup is shown in Fig. 1. A Perkin-Elmer TGA7 thermogravimetric analyzer was used for the thermal decomposition measurement. The main components of the system were a sensitive ultra-microbalance which provided a precise means of measuring weight (as small as 0.1 μg) from all runs, an alumina reactor with inlet and outlet, a movable furnace which had precise temperature control, and a computer to continuously record the mass variation of the sample with reaction temperature.

A platinum sample pan was used as a sample container to avoid any sample pan effect on the reaction. The effect of resistance to thermal and mass transfer on pyrolysis was eliminated by placing small amounts of specimen into the platinum sample pan. A known weight of sample of 8 ± 0.2 mg was employed for each experimental run. The sample pan was freely suspended on a suspension wire from a balance into a furnace tube. The reaction temperature was controlled by a standard platinum–rhodium thermocouple close to the sample. The nitrogen gas passed through the tube from top to bottom. To avoid contamination of residual impurities within the system, the flow rate of gas was first introduced at a large rate of flow, and then fixed at 60 ml/min. The N_2 flow rate was monitored with a mass-flow meter. All experiments were performed under non-isothermal conditions at temperatures between 300 and 1300 K, using heating rates of 5, 10, 15 and 20 K/min. Several tests were performed to ensure that the sampling technique employed was valid. The degree of conversion of electronic packaging material pyrolyzed in N_2, X, is defined here as

$$X = \frac{W_0 - W}{W_0 - W_\infty} \tag{1}$$

where W_0, W and W_∞ represent initial, instantaneous and final masses of sample, respectively. Once the three masses had been read from TGA, the conversion (X) was readily obtained according to a simple calculation.

2.3. Analysis of metallic impurities and organic elements

To measure the amount of metallic impurities in the samples, the reactant and product after pyrolysis were dissolved in a solution of HNO_3 and HF, and heated at 453 K for 6 h. Then the amounts of metallic impurities in the solution were determined with an inductively coupled plasma-mass spectrometer (ICP-MS) (Kontron Plasmakon, model S-35). The amounts of fundamental organic element treated with various heating rates were determined using a Heraeus elemental analyzer. The dried sample was powdered to 325 mesh size (ASTM), and this powder was employed in the analysis.

2.4. Analysis of physical properties

X-ray diffractograms were recorded with a diffractometer (Siemens, model D-500) using Cu Kα radiation, for the determination of the crystalline structure of the reactant and

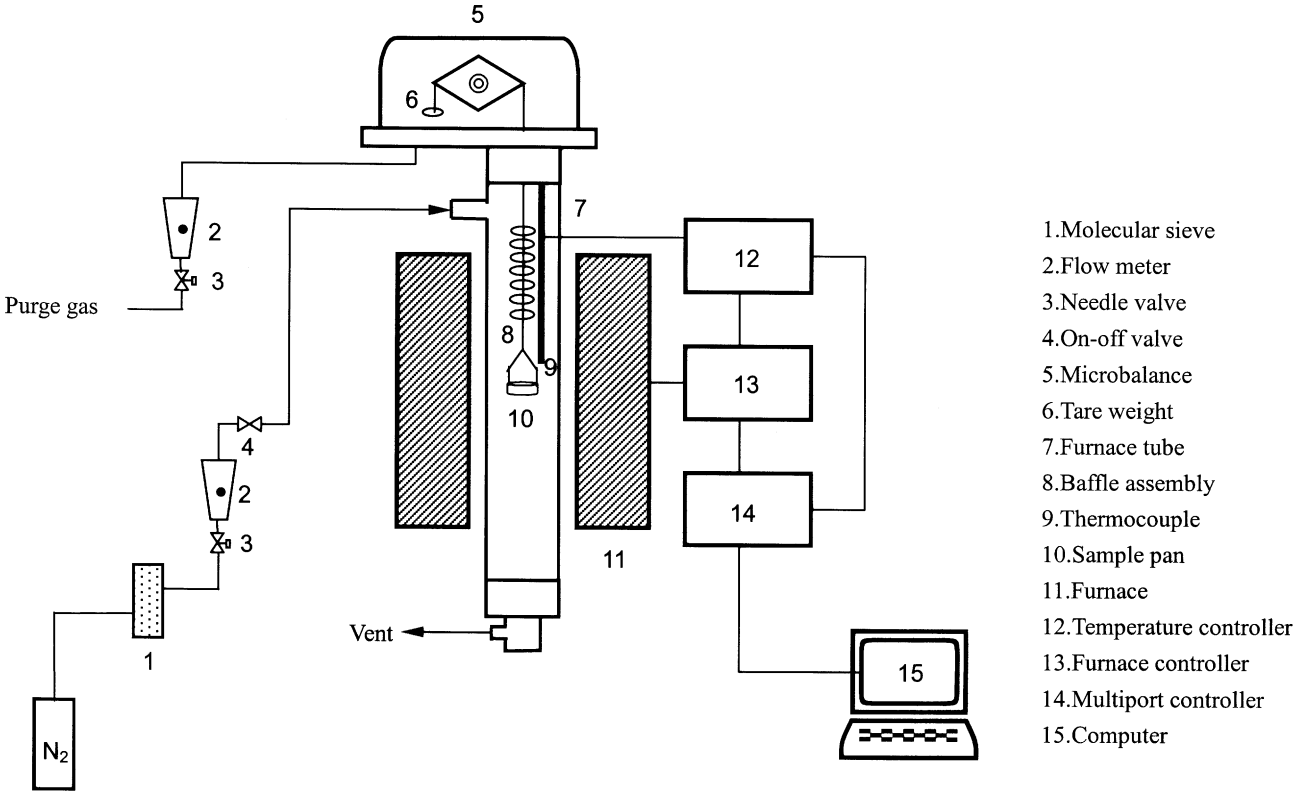

Fig. 1. Schematic diagram of the experimental apparatus for pyrolysis of electronic packaging material.

product at various heating rates. The scanning rate was $2.5^{\circ}\,min^{-1}$. Morphological features of reactant and product were obtained with a scanning electron microscope (Topcon, model ABT-150S). A N_2 adsorption analyzer (Micrometric, model ASAP 2000) was used to investigate the Brunauer–Emmett–Teller (BET) surface area, pore volume, and average pore diameter of the samples. Each sample was outgassed at 378 K for 1 h in the N_2 adsorption apparatus prior to any adsorption–desorption cycle. Samples pyrolyzed at various heating rates in the region of 400–4000 cm^{-1} were measured using an infrared spectrometer (Shimadzu, model FTIR-8300).

3. Results and discussion

3.1. Analysis of metallic impurities and organic elements

The amounts of metallic ingredients present in the water-rinse and various heating rates samples are given in Table 2. The main metallic impurities present in samples were antimony, iron, sodium, aluminum and chromium; of which the concentration of antimony was greatest. Compared with the water-rinsed sample, the impurity content was significantly reduced by the pyrolysis process. About 77% of impurities were extracted after treatment of the sample by pyrolysis. For various heating rates, the total residual amount of metallic ingredients from a high heating rate is smaller than that from a low one. The decreased impurities may result from volatilization of organic matter, after which the metals were carried out from the volatiles during pyrolysis. Iji and Ikuta [8] reported that the antimony compound in electronic packaging material was very hard to remove because the compound had melted into the silica during the thermal decomposition.

Table 3 shows the relationship between heating rate and the amount of organic element remaining in the pyrolyzed samples. The water-rinsed sample can be regarded as consisting of 80.22 wt.% ash, 15.95 wt.% carbon, 1.98 wt.% hydrogen, 1.68 wt.% oxygen and 0.17 wt.% nitrogen. The residual amount of organic matter in the water-rinsed sample was greater than that in the pyrolyzed samples. However, on the other hand the percentage of ash in the pyrolyzed samples increased. This ash contains >95% silica and is an important renewable source of silica [8].

Table 2
Amount of metallic ingredients in the electronic packaging material before and after pyrolysis samples

β (K/min)	Metallic ingredients as oxides (ppm)										
	Sb	K	P	Au	Fe	Na	Mg	Al	Cr	Ag	Total
0[a]	11800	<8	96	<8	5780	240	53	3140	1580	<8	22713
5[b]	4240	<8	<8	<8	107	304	128	456	14.4	<8	5281.4
10[b]	4240	<8	<8	<8	86.4	61.7	123	447	12.3	<8	5002.4
15[b]	3730	<8	<8	<8	122	82	119	358	13.4	<8	4456.4
20[b]	3420	<8	<8	<8	108	101	155	443	11.6	11.6	4274.2

[a] Sample was water-rinsed and unpyrolyzed.
[b] Sample was pyrolyzed in a nitrogen atmosphere.

Table 3
Elemental composition of the electronic packaging material before and after pyrolysis samples

β (K/min)	Composition (wt.%)				
	C	H	O	N	Ash
0[a]	15.95	1.98	1.68	0.17	80.22
5[b]	7.20	0.46	0.13	0.08	92.13
10[b]	7.53	0.37	0.38	0.09	91.63
15[b]	7.23	0.35	0.85	0.10	91.47
20[b]	7.52	0.43	0.75	0.06	91.24

[a] Sample was water-rinsed and unpyrolyzed.
[b] Sample was pyrolyzed in a nitrogen atmosphere.

3.2. Analysis of physical properties

Fig. 2 shows the nitrogen adsorption–desorption isotherm of electronic packaging material before and after pyrolysis in a N_2 atmosphere. The lower portion of the loop is traced out on adsorption, the upper portion on desorption. A hysteresis loop, associated with capillary condensation at P/P_0 above 0.45, is shown in Fig. 2(a), which indicates that the pyrolyzed product is a porous material. Fig. 2(b) shows no hysteresis loop for adsorption and desorption of nitrogen on the original sample, indicating that the pore diameters are all non-porous or macroporous. The isotherm is convex over the entire range, indicating that the forces of adsorption between adsorbate and adsorbent are relatively weak [12].

The pore size distribution, as determined by the Barrett–Joyner–Halenda (BJH) method [13] (based on the desorption branch), is shown in Fig. 3. This result is a plot of the increment of pore volume per increment in pore size, versus pore size. Fig. 3(a) shows a narrow pore size distribution for the pyrolyzed sample, with most of the pores being about 4 nm in diameter, referred to as mesopores. Fig. 3(b) shows a wide pore size distribution for the original material, with most of the pores being larger than 50 nm, referred to as macropores.

The results of surface area and pore structure of sample pyrolyzed at various heating rates are listed in Table 4. The BET method [14] is used for the analysis of specific surface area. Comparing before and after pyrolysis, the specific surface area is clearly increased from 1.09 to 63.38 m^2/g. The pyrolyzed samples are highly porous materials which have a larger internal surface area. This is mainly attributed to the resin matter having been broken

Table 4
Surface area and pore characteristics of the electronic packaging material before and after pyrolysis samples

β (K/min)	BET surface area (m^2/g)	Total pore volume (ml/g)	Average pore diameter, $4V/A$ (Å)
0[a]	1.09	0.0028	103.26
5[b]	63.38	0.0339	21.38
10[b]	62.56	0.0335	21.39
15[b]	62.00	0.0330	21.28
20[b]	61.51	0.0328	21.35

[a] Sample was water-rinsed and unpyrolyzed.
[b] Sample was pyrolyzed in a nitrogen atmosphere.

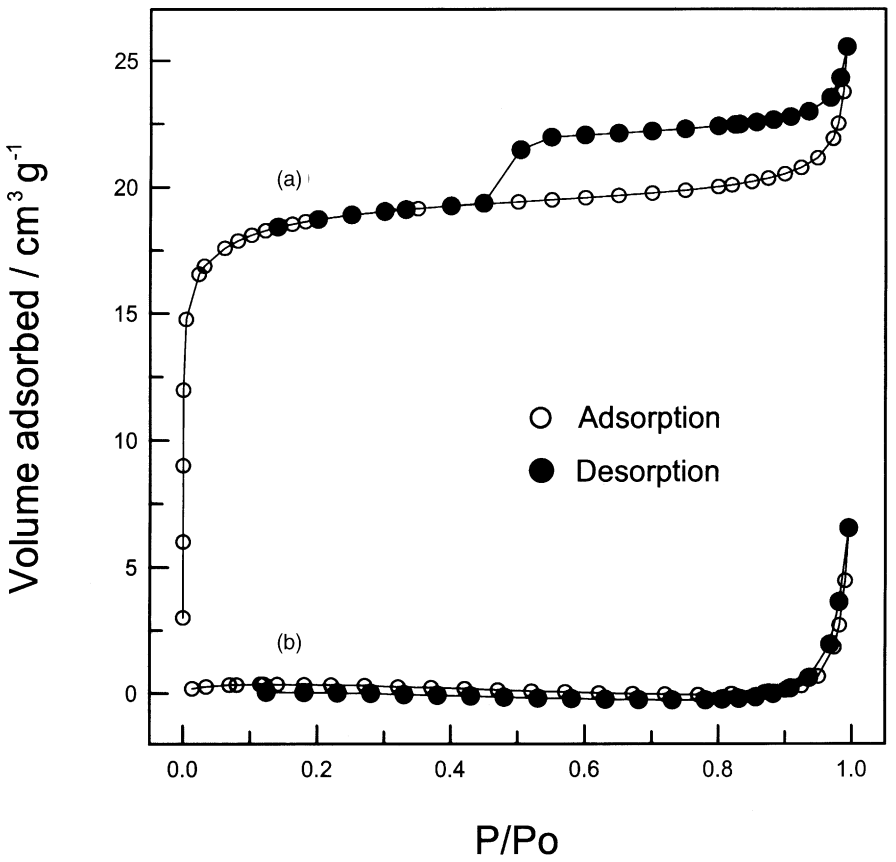

Fig. 2. Adsorption–desorption isotherms of nitrogen at 77 K before and after pyrolysis samples: (a) specimen was pyrolyzed at 5 K/min in N_2; (b) unpyrolyzed specimen.

up during the pyrolysis, thus leaving a highly porous structure and increasing the surface area. The table also indicates that the heating rates have a slight effect on the total specific surface area, with larger heating rate having lower specific surface area. This decrease possibly comes from a portion of pores having been destroyed when the heating rate is increased, therefore resulting in the decrease of specific surface area. As shown in Table 4, the total cumulative pore volume of the unpyrolyzed sample is 0.0028 ml/g, much smaller than that of pyrolyzed samples, which has an average value is 0.0333 ml/g. The average pore diameter (by BET) of unpyrolyzed sample is 103.26 Å, which is much larger than that of pyrolyzed samples, which have an average value of 21.35 Å.

Fig. 4 shows X-ray diffraction analysis of electronic packaging material before and after pyrolysis at various heating rates. There are no characteristic peaks present in Fig. 4(a), indicating that the original sample was completely an amorphous form. However, in the pyrolyzed samples (Fig. 4(b)–(e)), the characteristic of fused silica was observed in the XRD pattern, with a maximum of $2\theta = 22.5^{\circ}$. No crystalline silica was found in any of the runs.

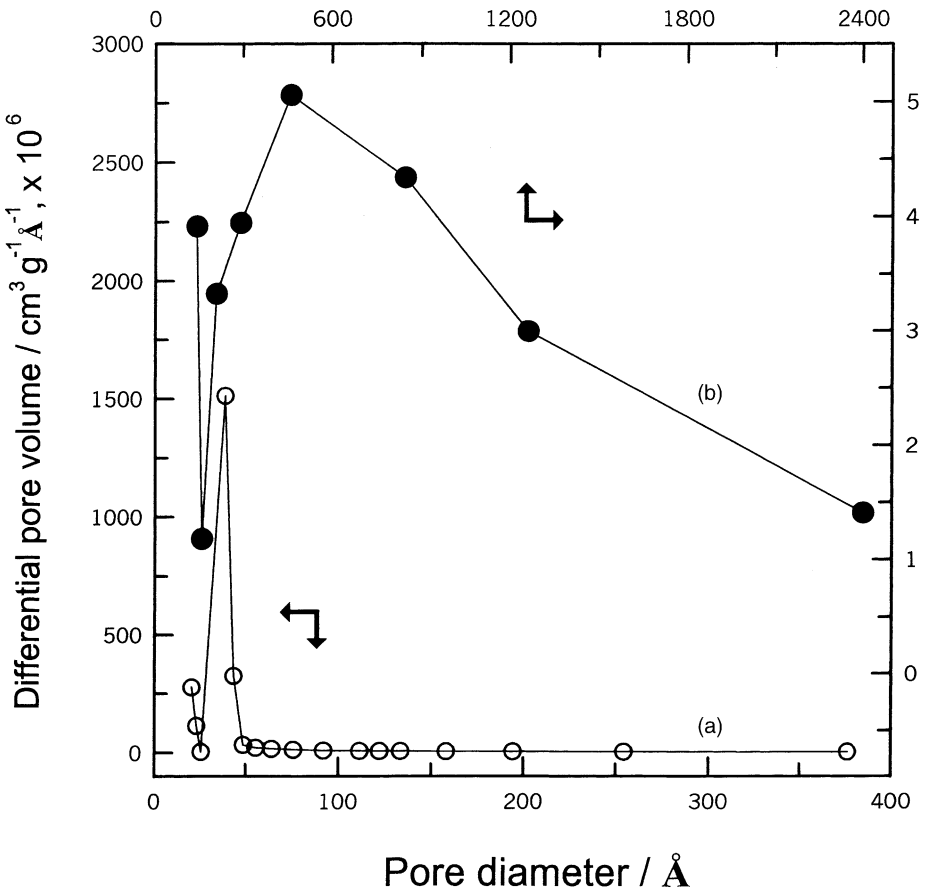

Fig. 3. Differential pore size distribution of the electronic packaging material calculated from the desorption isotherm by the BJH procedure: (a) specimen pyrolyzed at 5 K/min in N_2; (b) unpyrolyzed specimen.

Iji and Ikuta [8] reported that the fused silica, obtained from burning of electronic packaging material at 1273 K in air, is an amorphous form, which is consistent with the present study.

The FTIR pattern of the samples pyrolyzed at various heating rates is shown in Fig. 5. Similar spectra were obtained for the pyrolyzed samples which were coked under various heating conditions. In comparison with the spectrum of commercial grade silica, the absorption bands at ∼475, ∼805 and 1115 cm^{-1}, are indications of silica. For various heating rates, the intensity of the bands increases with decreasing heating rate.

As a general picture, Fig. 6(a) shows the apparent surface of molding residues of the electronic packaging material. The molding residues appear round, with branches on both sides. Fig. 6(b)–(d) are electron micrographs of products obtained by heating the sample in nitrogen at 5 K/min. Fig. 6(b) shows that some pores have been formed when the pyrolysis reaction is completed. The pores obtained by destruction of resin matter in the pyrolysis of electronic packaging material have a high pore volume and surface area, which is consistent

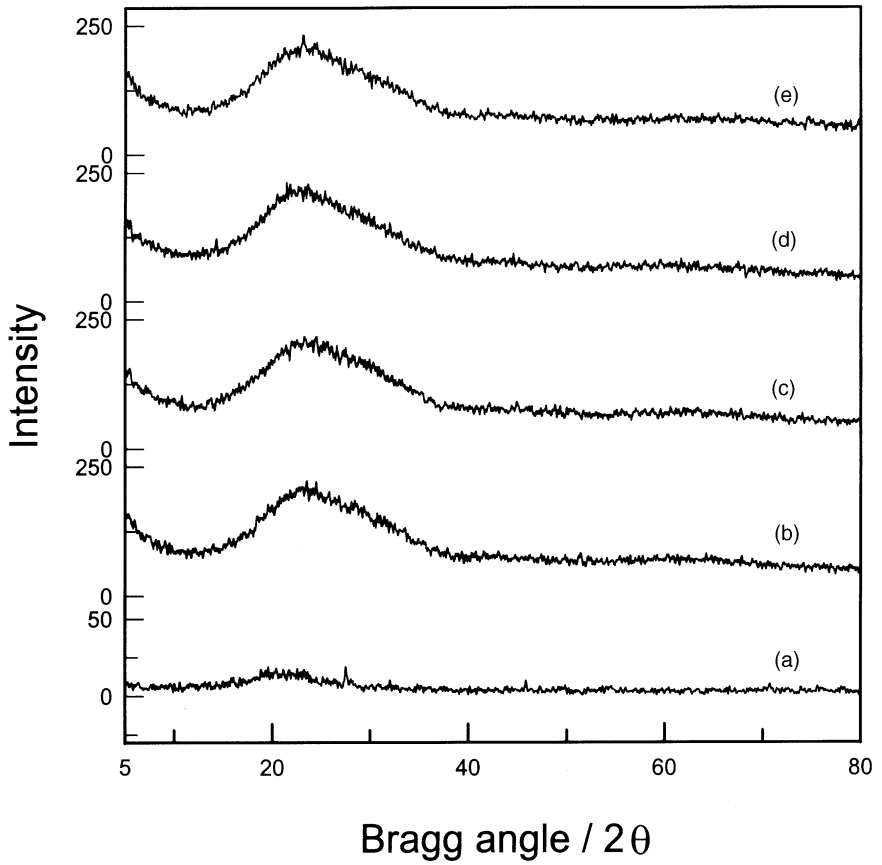

Fig. 4. X-ray diffractogram of electronic packaging material: (a) unpyrolyzed specimen; (b)–(e) specimens pyrolyzed at 5, 10, 15 and 20 K/min in N_2, respectively.

with the results of pore structure measurement, as indicated in Table 4. Fig. 6(c) indicates that the distribution of product is mainly in the form of irregular grains. The residue obtained by pyrolysis of electronic packaging material in nitrogen atmosphere is black. In addition, a portion of the product is spherical, as was also observed in the pyrolyzed specimen (Fig. 6(d)). The spherical shape of product is the molding filler of silica. The same structural features had been reported by Iwasa et al. [15].

4. Kinetics analysis

4.1. Effect of temperature on pyrolysis

The variations in the conversion (X, TG curves) and the derivative of conversion (dX/dt, DTG curves), as a function of reaction temperature for the pyrolysis of electronic packaging

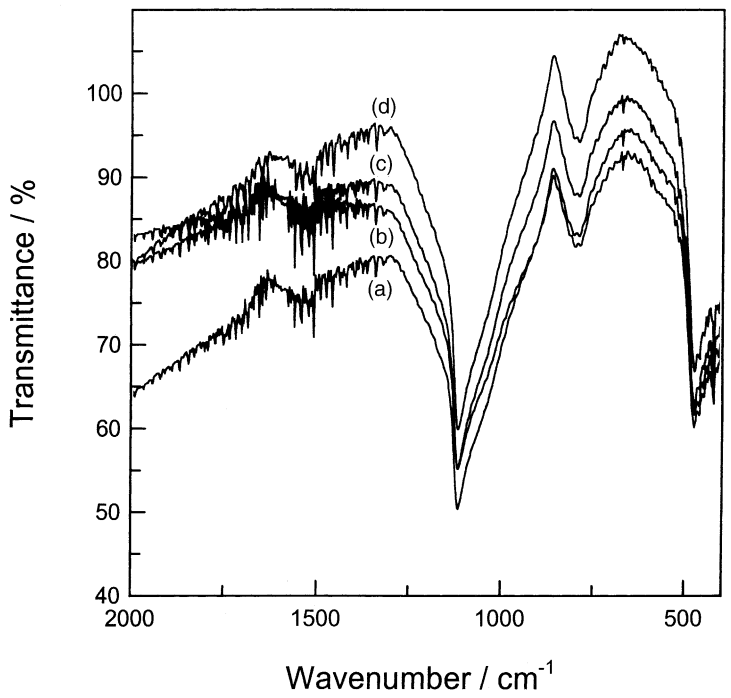

Fig. 5. FTIR spectrogram of electronic packaging material: (a)–(d) specimens pyrolyzed at 5, 10, 15 and 20 K/min in N_2, respectively.

material are shown in Fig. 7. The samples are fired at heating rates of 5, 10, 15 and 20 K/min in a nitrogen atmosphere.

In the TG curves from Fig. 7, the conversion effect appears in the samples pyrolyzed at 400–1200 K. This conversion increase is attributed to the removal of combustible volatiles. It is observed that there is one inflection point shown on the TG curves, indicating that the pyrolysis of electronic packaging material takes place in two main stages. For the same temperature of pyrolysis, the retention time for specimen to decomposition increases as the heating rate decreases, thus promoting the conversion. Chen and Yeh [16] reported the pyrolysis of epoxy resin in N_2, and also obtained the same tendency. From Fig. 7, the conversion is changed in the first stage from 0 to 0.56 and in the second stage from 0.56 to 1.0 as the pyrolysis temperature is increased from 400 to 1200 K, respectively. The slope of the heating curves in the first stage is slightly larger than in the second stage, indicating that part of the reactant is not easily decomposed in the second stage. When the temperature exceeds 1200 K, the electronic packaging materials are almost completely decomposed to carbon, and a higher pyrolysis temperature does not further affect the loss of mass.

In the DTG curves from Fig. 7, there is just one peak observed in each heating rate, and this peak shifts to the high-temperature region when the heating rate increases. Furthermore, the height of the peak, which is associated with the instantaneous rate of conversion, also increases with increasing heating rate. In a previous study, Liou et al. [17] reported the

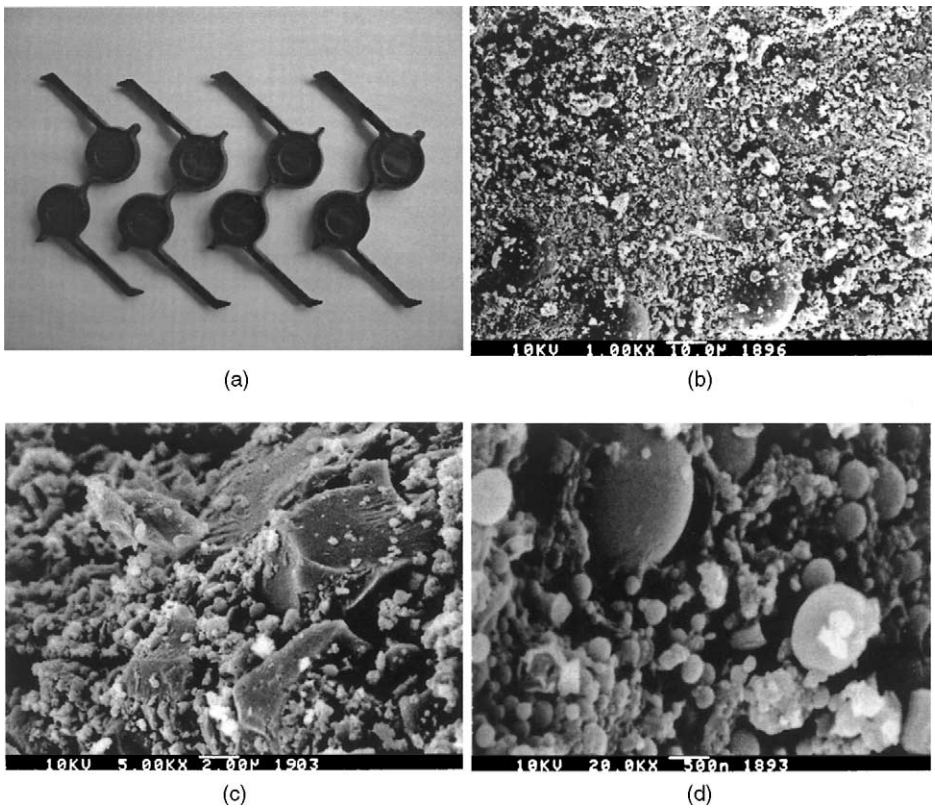

Fig. 6. Scanning electron micrographs of electronic packaging material: (a) raw material of unpyrolyzed specimen (taken as a general picture); (b) pyrolyzed specimen at 5 K/min in N_2 (1000×); (c) inner surface of pyrolyzed specimen at 5 K/min in N_2 (5000×); (d) inner surface of pyrolyzed specimen at 5 K/min in N_2 (20,000×).

pyrolysis kinetics of rice husk in nitrogen atmosphere, and also obtained the same conclusion. According to the results in Fig. 7, the main pyrolysis temperature of the electronic packaging material is clearly in the range of 609–628 K.

The pyrolysis characteristics of electronic packaging material are summarized in Table 5. In the reaction temperature range, a continuous increase in both initial (T_i) and final (T_f) reaction temperatures, with increasing heating rate, is obtained. Because T_f increases more

Table 5
Reaction characteristics of the electronic packaging material

β (K/min)	T_i (K)	T_m (K)	T_f (K)	ΔT (K)	W_∞/W_0 (%)
5	407.1	609.3	1158.5	751.4	89.3
10	412.8	618.7	1180.7	767.9	89.0
15	419.5	622.7	1197.1	777.6	88.9
20	419.8	628.7	1208.0	788.2	88.7

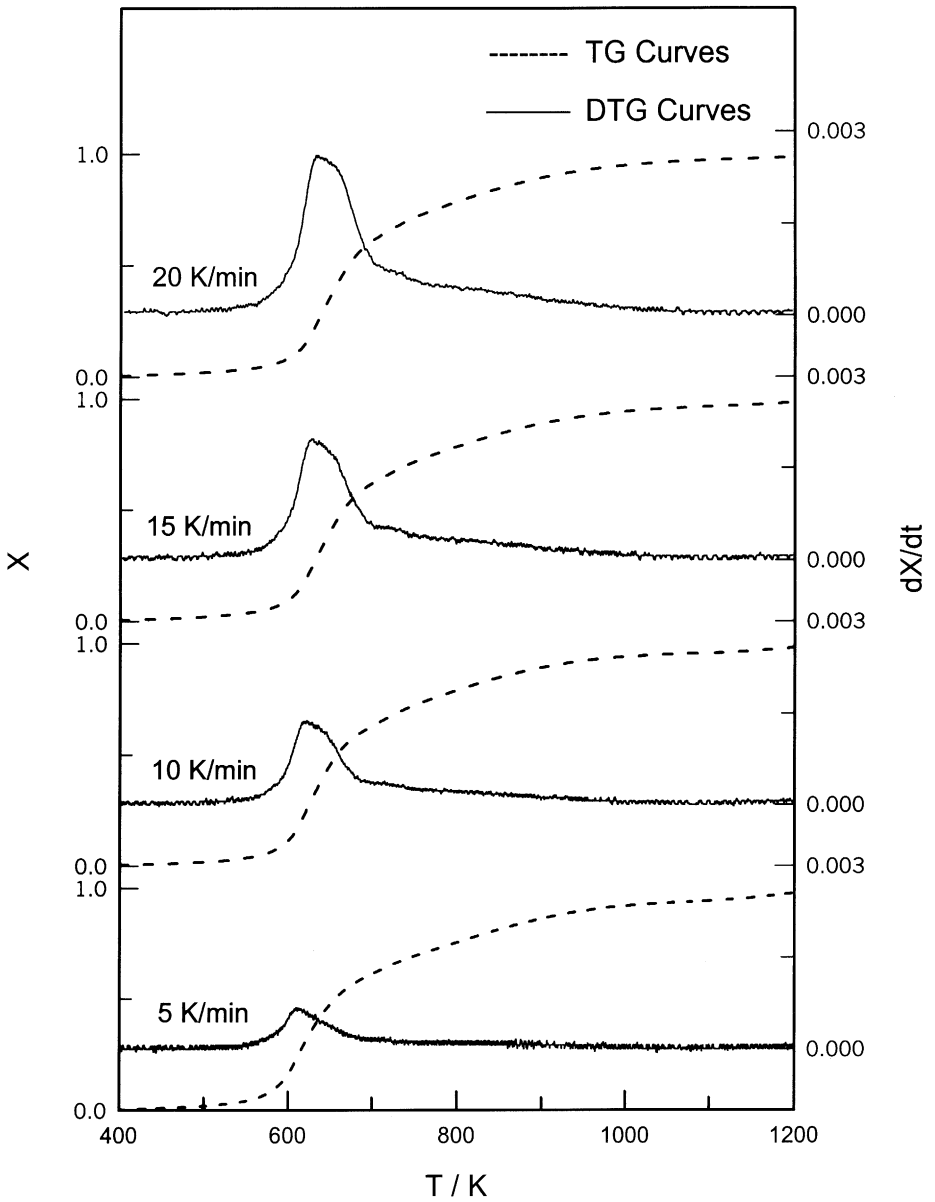

Fig. 7. Effect of heating rate on the pyrolysis of the specimen: nitrogen flow rate, 60 ml/min; sample loading, 8 mg; initial grain size, 38–45 μm.

than T_i, the reaction range ($\Delta T = T_f - T_i$) also increases with increasing heating rate. Table 5 shows that the initial reaction temperature changes from 407 to 419 K, the final reaction temperature changes from 1158 to 1208 K, and the peak temperature (T_m) at which derivative of conversion is maximum changes from 609 to 628 K. It is also seen from Table 5

that the fractional residual (W_∞/W_0) of electronic packaging material decreases from 89.3 to 88.7 wt.% as the heating rate is increased from 5 to 20 K/min.

4.2. Activation energy

In this study, the Friedman method [18] is employed to evaluate the apparent kinetic parameters E, A and n of pyrolyzed electronic packaging material from the TG data. The derivation of kinetic data also refers to other related theory [19–22].

The rate of conversion in pyrolysis, dX/dt, can be represented by the following equation:

$$\frac{\mathrm{d}X}{\mathrm{d}t} = kf(X) \tag{2}$$

The reaction rate constant, k, is expressed according to the Arrhenius equation

$$k = A\exp\left(-\frac{E}{RT}\right) \tag{3}$$

where A is the pre-exponential factor, E the activation energy, and T the reaction temperature, respectively. A function of conversion independent of temperature, $f(X)$, is expressed as

$$f(X) = (1 - X)^n \tag{4}$$

Substituting Eqs. (3) and (4) into Eq. (2) and taking a natural logarithm yields

$$\ln\left(\frac{\mathrm{d}X}{\mathrm{d}t}\right) = \ln[A(1 - X)^n] - \frac{E}{R}\frac{1}{T} \tag{5}$$

Based on Eq. (5), the plot of instantaneous rates (ln(dX/dt)) versus temperature ($1/T$) from Fig. 7 at various heating conditions yields a straight line. The values of activation energy, E, which are obtained from the slopes of the straight lines, are shown in Fig. 8, as a function of conversion. The activation energies for nitrogen pyrolysis of electronic packaging material may be divided into three groups. The three average activation energy values are $E = 153 \pm 15$ kJ/mol for $X = 0$–0.56, $E = 251 \pm 10$ kJ/mol for $X = 0.56$–0.70, and $E = 127 \pm 10$ kJ/mol for $X = 0.70$–1.0.

Furthermore, the plot of $\ln[A(1-X)^n]$ against $\ln(1-X)$ yields a least-squares straight line, and from the slope and intercept of the straight line, the reaction order (n) and pre-exponential factor (A) are also obtained. The kinetic parameters of electronic packaging material pyrolyzed in nitrogen are summarized in Table 6, which shows the activation energy (E), pre-exponential factor (A) and reaction order (n) in two reaction stages.

Table 6
Kinetic parameters for pyrolysis of the electronic packaging material

	First stage	Second stage	
	$X = 0$–0.56	$X = 0.56$–0.70	$X = 0.70$–1.0
E (kJ/mol)	153 ± 15	251 ± 10	127 ± 10
A (min^{-1})	3.55×10^{10}	7.78×10^{15}	1.58×10^{5}
n	1.5	1.0	1.0

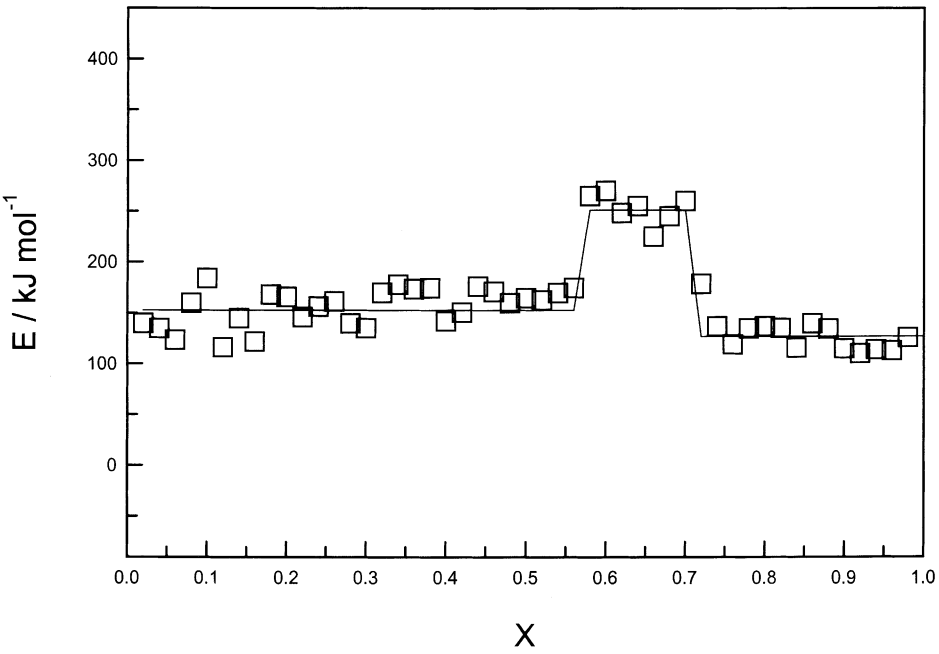

Fig. 8. Calculated activation energies at different conversions for pyrolysis of the specimen.

Chen and Yeh [16] postulated that the average activation energy from the pyrolysis of epoxy resin in a nitrogen atmosphere is 173 kJ/mol. Liu et al. [23] determined that the values of the activation energy (according to Friedman's method), by thermal decomposition of phosphorus-containing epoxy resin in nitrogen, are 179 kJ/mol for the first-stage reaction and 196 kJ/mol for the second stage reaction, respectively. These values are lower than those obtained in the present study. One possible reason for this is that the activation energy contributed by thermal decomposition of phenol resin in electronic packaging material is higher than that of pure epoxy resin [24].

4.3. Thermal decomposition mechanism

The observed features of the pyrolysis of electronic packaging material can be explained on the basis of the decomposition behavior of its major constituents: epoxy resin, phenol resin and ash (mostly silica). In the present investigation, three groups of activation energy values are obtained. In the first stage reaction (conversion 0–0.56), there is only one average activation energy observed. However, there are two components of resin matter (mainly epoxy resin and phenol resin) present in the first stage, indicating that there is a superposition of the decomposition of epoxy resin and phenol resin. In the second stage (conversion 0.56–1.0), there are two average activation energies observed. Hence, the pyrolysis mechanism of electronic packaging material in that stage is composed of more than one reaction. The two average activation energies in the second stage are attributed to the

further pyrolysis of two intermediates, which are noted as residual resin matter from the epoxy resin and phenol resin in the first stage. In addition, it can be clearly observed that the volatilization of gas products is accompanied by the formation of tar during the pyrolysis reaction.

A reasonable assumed mechanism is proposed to describe the pyrolysis process of electronic packaging material in the following scheme:

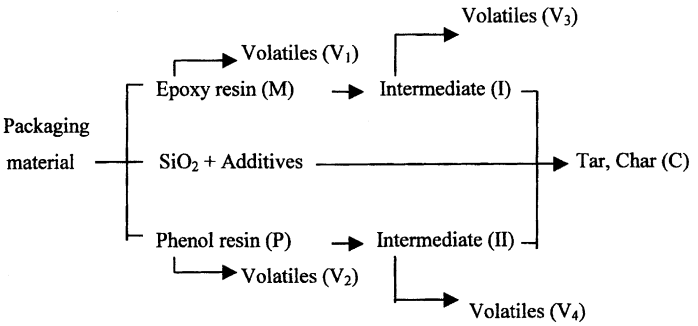

In this scheme, the pyrolysis process at the first stage includes decomposition of epoxy resin (M) and phenol resin (P) into the individual intermediates (I and II), which may be organic material of smaller molecular weight; then both gaseous volatiles (V_1 and V_2) were released from individual pyrolysis reactants (M and P). In the second stage, the intermediates (I and II) continue with further pyrolysis to form other volatile species (V_3 and V_4), tar and char (C). The final char is composed of a mixture of carbon and silica. The first stage of pyrolysis is mainly due to the side-group elimination and main-chain scission of the original resin constituents, and yields combustible volatiles and intermediates. The second stage of pyrolysis is associated with the dehydration or breakdown of residual resin components (or intermediates) that decompose to yield gas and the char. From the above observation, we can conclude that there are two competitive reactions contained in the mechanism, so the thermal decomposition of epoxy resin and phenol resin in the electronic packaging material results in the formation of carbon, silica, tar and gas volatiles.

Other researchers [16,23,25] reported one or two stages for decomposition of plastic materials such as epoxy resin, with a consistent qualitative description that the major loss of mass during degradation is attributed to evolution of volatile matter, with further decomposition to char or tar. Because the major constituent of electronic packaging materials is more than one resin component, the pyrolysis reaction is complicated, with more than one pathway of chemical decomposition observed in the present work.

5. Conclusions

Pyrolysis kinetics of electronic packaging material in a nitrogen atmosphere at the heating conditions of 5, 10, 15 and 20 K/min are described. The corresponding kinetic parameters such as activation energy, pre-exponential factor, and reaction order are determined. About 77% of impurities are extracted after pyrolysis of the samples. Detailed information about

the pore structure characteristics of specific surface area, pore volume and pore diameter are discussed. The results of thermogravimetric analysis reveal that two reaction stages are included in the pyrolysis system. The initial, final reaction temperature and reaction range, all increase when the heating rate is increased. The activation energy can be divided into three groups. The observed thermal behavior is explained on the basic of two competitive reactions, degradation of epoxy and phenol resins, which are the major resin constituents of electronic packaging material. The final products are carbon, silica, tar and gas volatiles. The results of the study are useful for the rational design and operation of pyrolysis or incineration systems in which plastic waste from electronic components are involved, thus helping to solve the disposal and pollution problems.

Acknowledgements

The author expresses thanks to the National Science Council of Taiwan for its financial support under Project no. NSC 90-2214-164-001.

References

[1] A. Harper, Electronic Packaging and Interconnection Handbook, McGraw-Hill, New York, 1991, Chapter 6.
[2] H.Y. Chang, Y.T. Huang, M.S. Jing, K.L. Cheng, Japanese Patent JP 2000109650 (2000).
[3] W.R. Creasy, Polymer 33 (1992) 4486.
[4] J. Unsworth, Y. Li, J. Appl. Polym. Sci. 46 (1992) 1375.
[5] N. Rose, M.L. Bras, R. Debbol, B. Costes, Y. Hentry, Polym. Degrad. Stab. 42 (1993) 307.
[6] J.F. Lin, C.F. Ho, S.K. Huang, Polym. Degrad. Stab. 67 (2000) 137.
[7] T.H. Liou, in: Proceedings of the 2002 CIChE Annual Meeting and Conference, Taiwan, 2002, p. 97.
[8] M. Iji, Y. Ikuta, J. Environ. Eng. 124 (1998) 821.
[9] P. Budrugeac, Thermochim. Acta 221 (1993) 229.
[10] T.H. Liou, F.W. Chang, Ind. Eng. Chem. Res. 34 (1995) 118.
[11] F.W. Chang, T.H. Liou, F.M. Tsai, Thermochim. Acta 354 (2000) 71.
[12] C.N. Satterfield, Heterogeneous Catalysis in Industrial Practice, 2nd ed., McGraw-Hill, New York, 1991, Chapter 5.
[13] E.P. Barrett, L.G. Joyner, P.C. Halenda, J. Am. Chem. Soc. 73 (1951) 309.
[14] S. Brunauer, P.H. Emmett, E. Teller, J. Am. Chem. Soc. 60 (1938) 309.
[15] M. Iwasa, K. Yamamoto, K. Takahashi, Japanese Patent JP 08245214 (1996).
[16] K.S. Chen, R.Z. Yeh, J. Hazard. Mater. 49 (1996) 105.
[17] T.H. Liou, F.W. Chang, J.J. Lo, Ind. Eng. Chem. Res. 36 (1997) 568.
[18] H.L. Friedman, J. Polym. Sci.: Part C 6 (1964) 183.
[19] W.W. Wendlandt, Thermal Methods of Analysis, Wiley/Interscience, New York, 1974.
[20] M.J. Antal, H.L. Friedman, F.E. Rogers, Comput. Sci. Technol. 21 (1980) 141.
[21] H. Nishizaki, K. Yoshida, J.H. Wang, J. Appl. Polym. Sci. 25 (1980) 2869.
[22] Z.S. Petrovic, Z.Z. Zavargo, J. Appl. Polym. Sci. 32 (1986) 4353.
[23] Y.L. Liu, G.H. Hsiue, C.W. Lan, Y.S. Chiu, Polym. Degrad. Stab. 56 (1997) 291.
[24] J. Hetper, M. Sobera, J. Chromatogr. A 833 (1999) 277.
[25] J. Vogt, Thermochim. Acta 85 (1985) 407.